

Formation of *N*-Nitrosodimethylamine during Chloramination of Secondary and Tertiary Amines: Role of Molecular Oxygen and Radical Intermediates

Stephanie Spahr,^{†,‡,||} Olaf A. Cirpka,[⊥] Urs von Gunten,^{†,‡,§} and Thomas B. Hofstetter^{*,†,§,ID}

[†]Eawag, Swiss Federal Institute of Aquatic Science and Technology, CH-8600 Dübendorf, Switzerland

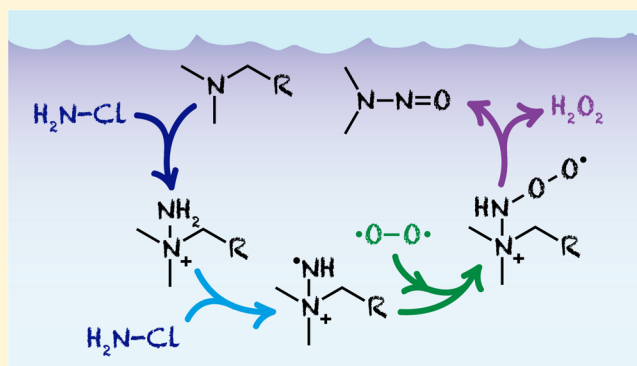
[‡]School of Architecture, Civil and Environmental Engineering (ENAC), Ecole Polytechnique Fédérale de Lausanne (EPFL), CH-1015 Lausanne, Switzerland

[⊥]Center for Applied Geoscience, University of Tübingen, D-72074 Tübingen, Germany

[§]Institute of Biogeochemistry and Pollutant Dynamics, ETH Zurich, CH-8092 Zurich, Switzerland

Supporting Information

ABSTRACT: *N*-Nitrosodimethylamine (NDMA) is a carcinogenic disinfection byproduct from water chloramination. Despite the identification of numerous NDMA precursors, essential parts of the reaction mechanism such as the incorporation of molecular O₂ are poorly understood. In laboratory model systems for the chloramination of secondary and tertiary amines, we investigated the kinetics of precursor disappearance and NDMA formation, quantified the stoichiometries of monochloramine (NH₂Cl) and aqueous O₂ consumption, derived ¹⁸O-kinetic isotope effects (¹⁸O-KIE) for the reactions of aqueous O₂, and studied the impact of radical scavengers on NDMA formation. Although the molar NDMA yields from five *N,N*-dimethylamine-containing precursors varied between 1.4% and 90%, we observed the stoichiometric removal of one O₂ per *N,N*-dimethylamine group of the precursor indicating that the oxygenation of N atoms did not determine the molar NDMA yield. Small ¹⁸O-KIEs between 1.0026 ± 0.0003 and 1.0092 ± 0.0009 found for all precursors as well as completely inhibited NDMA formation in the presence of radical scavengers (ABTS and trolox) imply that O₂ reacted with radical species. Our study suggests that aminyl radicals from the oxidation of organic amines by NH₂Cl and *N*-peroxyl radicals from the reaction of aminyl radicals with aqueous O₂ are part of the NDMA formation mechanism.



INTRODUCTION

N-Nitrosodimethylamine (NDMA) and other *N*-nitrosamines are potent carcinogens that can be formed as disinfection byproducts (DBPs) during chlorination, chloramination, and ozonation of drinking water and wastewater.^{1–5} Despite the identification of numerous NDMA precursor compounds and suggestions for NDMA mitigation under different treatment conditions,^{2,6–17} many aspects of the reaction mechanisms leading to NDMA remain elusive. In fact, the chloramination of amine-containing organic compounds has been identified as a major source of *N*-nitrosamines.^{2,18,19} Secondary amines such as dimethylamine (DMA) are reported as frequently occurring NDMA precursors with molar NDMA yields of up to 4%.^{20–22} Similar yields (<6%) observed during chloramination of tertiary amines with *N,N*-dimethylamine functional groups were interpreted as evidence for their transformation to secondary amines prior to NDMA formation.^{8,19–21,23–25} However, NDMA yields are substantially higher (>60%) if the tertiary *N,N*-dimethylamine moiety is bound via one methylene group to a (hetero)aromatic ring such as in the pharmaceutical

ranitidine.^{8,20,26–28} These high yields suggest that secondary amines are probably not central intermediates in reactions leading to NDMA. It remains unclear, however, whether differing NDMA yields from secondary and tertiary amines indeed reflect differing reaction mechanisms.

To date, there is only limited understanding of how NDMA is formed during the reaction of chloramine with tertiary amines. Based on the detection of cationic dimethylhydrazine intermediates during chloramination of ranitidine, Le Roux et al. proposed that NH₂Cl is attacked through nucleophilic substitution by the tertiary amine moiety of the precursor compound.²⁹ Moreover, the extent of NDMA formation depends on the molecular structure of the tertiary amine.^{27,30} Heterolytic bond dissociation energies for the elementary reaction to NDMA suggest that leaving groups capable of

Received: September 21, 2016

Revised: November 14, 2016

Accepted: November 22, 2016

Published: November 22, 2016

forming stable carbocations (e.g., methylfuranes) are key for high yields of NDMA.^{27,30} These studies provide important evidence for the initial chloramination reaction and possible factors influencing the formation of NDMA. However, information about the consumption of NH_2Cl and O_2 in central reactions, such as the incorporation of aqueous O_2 into the N–O bond of NDMA, is scarce and mainly circumstantial due to the challenges of characterizing transient reactive (oxygen) intermediates.

Regardless of the yield of NDMA formation during chloramination, reactions of aqueous O_2 play an important role in the NDMA formation pathway. Whereas chloramination experiments with ^{18}O -labeled H_2O showed no incorporation of ^{18}O into NDMA, the amount of NDMA formed increased with increasing concentrations of aqueous O_2 .^{22,26} Although thermodynamically feasible, elementary reactions of ground state triplet oxygen ($^3\text{O}_2$) with even-electron species such as the known NDMA precursors are spin forbidden and thus too slow to lead to the oxygenation of organic amines or NH_2Cl .^{31–34} As a consequence, molecular O_2 can only react after activation to singlet oxygen ($^1\text{O}_2$), through reduction to superoxide ($\text{O}_2^{\bullet-}$), or in reactions with radical species.^{31,34–36} Previous work suggests that the latter is the most likely option for NDMA formation during chloramination because neither the addition of β -carotene as $^1\text{O}_2$ scavenger nor the addition of superoxide dismutase as $\text{O}_2^{\bullet-}$ quencher had an effect on NDMA formation during chloramination of DMA.²² In contrast, formation of NDMA through radical intermediates has been proposed for breakpoint chlorination of DMA³⁷ as well as for chloramination of quaternary amines.³⁸ But direct experimental evidence for radical reactions with aqueous O_2 is still lacking.

The goal of this study was to elucidate the reactions of aqueous O_2 and NH_2Cl with regard to contributions of radical intermediates to NDMA formation during chloramination. To this end, we performed laboratory experiments with five NDMA precursor compounds, namely ranitidine, 5-(dimethylaminomethyl)furfuryl alcohol (DFUR), *N,N*-dimethylbenzylamine (DMBA), 2,4,6-tris(dimethylaminomethyl)phenol (TDMAP), and dimethylamine (DMA). Evidence for potential NDMA formation mechanisms was obtained from (i) the kinetics of precursor disappearance and NDMA formation, (ii) the quantification of aqueous O_2 and NH_2Cl consumption, (iii) the analysis of oxygen isotope fractionation of aqueous O_2 , and (iv) the study of the impact of radical scavengers on NDMA formation. We used the analysis of oxygen isotope ratios ($^{18}\text{O}/^{16}\text{O}$) of aqueous O_2 for the first time in the context of DBP formation. This methodology is well established for studies on activation of oxygen in enzymes and by transition metal complexes^{39–42} and reveals the mechanisms of O_2 activation from the magnitude of ^{18}O -kinetic isotope effects.

■ EXPERIMENTAL SECTION

Chemicals. A list of all chemicals including suppliers and purities is provided in the [Supporting Information](#) (SI). Monochloramine (NH_2Cl) stock solutions (30 mM) were prepared daily by mixing hypochlorite and ammonium chloride at pH 9.5 (molar Cl:N ratio of 1:1.05) as described previously.^{43,44}

Chloramination Experiments. Chloramination experiments were carried out with five NDMA precursors as listed in the [Introduction](#) section. Unless stated otherwise, reactors contained 10 mM phosphate buffer at pH 8.0 in amber glass bottles of volumes between 100 and 1000 mL. Organic amines

were added from either methanolic, ethanolic, or aqueous stock solutions to reach initial concentrations of 15 μM (see [Figure S4](#)). Reactions were initiated by addition of NH_2Cl in 15- to 18-fold excess corresponding to initial concentrations of 225–270 μM . For concentration analysis and reaction product identification, 1 mL of aqueous sample was withdrawn at selected time points and the reaction was quenched by adding 5 μL of a $\text{Na}_2\text{S}_2\text{O}_3$ solution (100 g/L). Na_2SO_3 was not used as a quencher owing to its reactivity with DFUR ([Figure S5](#)). NH_2Cl concentrations were quantified by either membrane introduction mass spectrometry (MIMS) or colorimetric methods (see [Chemical Analyses](#)). For continuous monitoring of the concentration of aqueous O_2 , we filled aliquots of the reaction solution in 11 mL amber glass vials that were closed without headspace with butyl rubber stoppers and aluminum crimp caps, and immersed a needle-type fiber-optic oxygen microsensor into each vial. Two types of control experiments were set up identically to assess the stability of the organic amine in the absence of NH_2Cl and to quantify the self-decay rate constant of NH_2Cl in the absence of the organic amine. Molar NDMA yields were calculated by dividing the measured concentration of NDMA by the initial concentration and the number of *N,N*-dimethylamine groups of the precursor.

To assess the reactivity of NH_2Cl with the furfuryl alcohol moiety of DFUR, we quantified the concentration of NH_2Cl during the reaction of 3 μM furfuryl alcohol with 45 μM NH_2Cl in 10 mM phosphate buffer at pH 8.0. To study the impact of radical scavengers on NDMA formation, we added either the hydroxyl radical scavenger *tert*-butanol (*t*-BuOH, 40 mM final concentration) or peroxy radical scavengers, namely 2,2'-azino-bis(3-ethylbenzothiazoline-6-sulfonic acid, ABTS, 2 mM) or *rac*-6-hydroxy-2,5,7,8-tetramethylchromane-2-carboxylic acid (trolox, 0.5 mM), to the reaction of DFUR (3 or 15 μM) with NH_2Cl (45 or 225 μM). Note that we refer to ABTS and trolox as reduced species of the radical scavengers. Experiments with radical scavengers differed regarding to the sequence of reactant addition and NH_2Cl quantification method. *t*-BuOH was spiked to a phosphate buffered solution containing DFUR before the addition of NH_2Cl . In contrast, ABTS was added immediately after spiking the DFUR-containing buffer with NH_2Cl . Trolox was dissolved in phosphate buffer to which DFUR as well as NH_2Cl were added. In the presence of *t*-BuOH and trolox, we quantified the NH_2Cl concentration with the ABTS method and MIMS, respectively. When ABTS was added as a radical scavenger, we observed the oxidation of ABTS to the colored $\text{ABTS}^{\bullet-}$ and used its absorbance to quantify the amount of consumed NH_2Cl indirectly ([Figure S21a](#)). Control experiments were set up to assess the reactivity of the organic amine or NH_2Cl with the radical scavengers.

To quantify the formation of H_2O_2 during the reaction of DFUR (50 μM) with NH_2Cl (750 μM), we filled the reaction solution into 11 mL amber glass vials that were closed headspace-free and monitored the decrease of O_2 concentration as described above. When the consumed O_2 was stoichiometrically equal to the initial nominal concentration of DFUR, we added 100 μL catalase from bovine liver (0.3 g L⁻¹ final concentration). The observed increase in aqueous O_2 concentration upon addition of catalase corresponds to half of the H_2O_2 concentration in the reactor. To assess the stability of H_2O_2 during the NDMA formation reaction, we added 50 μM H_2O_2 immediately after the reaction of DFUR (50 μM) with NH_2Cl (750 μM) was initiated and determined the recovery of H_2O_2 by addition of catalase after 3.3 h. A more

detailed description of experiments with catalase is provided in the SI (section S13).

Oxygen Isotope Fractionation Experiments. The fractionation of stable O isotopes of aqueous O₂ was studied in amber reactors containing a magnetic stir bar and 11 mL of a 3 mM NH₂Cl solution in 10 mM phosphate buffer (pH 8.0). The vessels were closed without headspace and an oxygen microsensor was introduced to measure continuously the concentration of aqueous O₂. 15 to 200 μM organic amine (ranitidine, DFUR, DMBA, or TDMAP) was added to the reactor while stirring to initiate the reaction. Once the amount of consumed O₂ equaled the initial nominal concentration of the added organic amine, the reaction was quenched by creating a N₂ headspace following the procedure of Pati et al.⁴⁵ To this end, 3 mL of solution was replaced by N₂ gas with a gastight glass syringe. Partitioning of O₂ to the N₂-headspace was promoted through horizontal shaking for 30 min at 200 rpm while keeping the vessels upside down. Control samples containing 3 mM NH₂Cl without organic amine or 200 μM organic amine without NH₂Cl were prepared similarly. Owing to much slower reaction kinetics of DMA and NH₂Cl, we prepared 12 replicate samples containing 200 μM DMA and 3 mM NH₂Cl as well as 12 control samples with 3 mM NH₂Cl. Two reactive batches and one control batch were processed at selected time points over a time period of 4 days. In experiments with DMBA, TDMAP, and DMA, we additionally determined the concentration of NDMA immediately after sample quenching in the withdrawn reaction solution.

Chemical Analyses. Concentrations of ranitidine, DFUR, and NDMA were quantified with reverse phase HPLC coupled to a UV–vis detector using previously described methods (see section S3 for details).²⁸ Analytical errors of the reported concentrations are typically <1%. Transformation products formed during chloramination of ranitidine and DFUR were analyzed by liquid chromatography-high-resolution tandem mass spectrometry (LC-HR-MS/MS) using an adjusted analytical method described in Gulde et al.⁴⁶ (see section S4 for details).

Quantification of Aqueous O₂. Concentrations of aqueous O₂ were continuously measured with needle-type fiber-optic oxygen microsensors connected to a 4-channel transmitter (PreSens Precision Sensing GmbH, Germany). Four oxygen sensors were operated simultaneously after daily calibration with air-saturated and oxygen-free water. O₂ concentrations were corrected for variations in temperature. The analytical uncertainties of O₂ concentrations were smaller than ±0.5 μM.

NH₂Cl Concentrations. Concentrations of NH₂Cl were determined by membrane introduction mass spectrometry (MIMS)⁴⁷ as well as spectrophotometrically using either ABTS or *N,N*-diethyl-*p*-phenylenediamine (DPD) with iodide (I[−]) as catalyst,^{48,49} or the indophenol method.⁵⁰ NH₂Cl does not react with ABTS but with I[−] to form hypoiodous acid, which oxidizes ABTS^{2−} to the colored ABTS^{•−}. A detailed description of the methods for NH₂Cl quantification can be found in section S5. A Varian Cary 100 Bio UV–visible spectrophotometer was used for colorimetric assays. MIMS analysis was performed using a MIMS 2000 (Microlab, Aarhus, Denmark) equipped with a multiport valve to enable an automatic measurement of multiple samples. The membrane inlet temperature was set to 40 °C and the sample flow rate was 4 mL min^{−1}. Steady-state signals of *m/z* 51 and *m/z* 53 were reached after 2 min and measured for 6–8 min. The software used for analysis of MIMS signals is described elsewhere.⁴⁷ We

used NH₂Cl calibration rows from either 10–50 μM or 50–300 μM. Note that ranitidine, DFUR, NDMA, and trolox did not produce any interfering signals in the mass spectrometer. In NDMA formation experiments, we detected an interference at *m/z* 51 that was presumably created from an unknown reaction intermediate (see Figure S2). In this case, quantification of NH₂Cl was performed at *m/z* 53. All reported NH₂Cl concentrations were corrected by the self-decay of NH₂Cl observed in controls containing chloramine only. Note that the four methods used for determining NH₂Cl concentrations led to differing results when NH₂Cl was quantified during NDMA formation (see discussion in section S5.3 and Figure S3). The total turnover of NH₂Cl determined at the end of these experiments was, however, identical (section S5).

Stable Oxygen Isotope Analysis. ¹⁸O/¹⁶O ratios of aqueous O₂ were measured with gas chromatography isotope ratio mass spectrometry (GC/IRMS) following recently developed procedures of Pati et al.⁴⁵ Briefly, sample vials to which a 3 mL N₂ headspace had been introduced were mounted on a CombiPAL autosampler (CTC Analytics) equipped with a 2.5 mL gastight headspace syringe. The syringe was flushed with N₂ gas for 1 min before withdrawing 250 μL of the headspace from the sample. The gaseous sample was injected into a split injector (5 mm ID quartz liner, 200 °C) of a Trace GC (Thermo Fisher Scientific) that was equipped with a Rt-Molsieve 5 Å PLOT column (Restek, 30 m × 32 mm ID, 30 μm film thickness at 30 °C) to separate O₂ from N₂. Helium (99.999%) was used as carrier gas at 80 kPa and the split flow was 40 mL min^{−1}. O₂ pulses were introduced into a GC combustion III interface (Thermo Fisher Scientific) equipped with a Nafion membrane for removal of water and subsequently entered a Delta Plus XL IRMS (Thermo Fisher Scientific).

O isotope ratios are expressed in the delta notation as δ¹⁸O in permil (eq 1) relative to Vienna Standard Mean Ocean Water (VSMOW). Sample sequences included standards generated from air-saturated phosphate buffer, which were measured in triplicates after every 6 samples to ensure accuracy of δ¹⁸O measurements in a standard bracketing procedure. Uncertainties of δ¹⁸O measurements were below ±0.5‰. Blank samples containing oxygen-free water were analyzed in triplicates at the end of each sequence for blank corrections of diffusive O₂ input during sample preparation and injection (see Pati et al.⁴⁵ for details).

$$\delta^{18}\text{O} = \frac{(^{18}\text{O}/^{16}\text{O})_{\text{sample}}}{(^{18}\text{O}/^{16}\text{O})_{\text{VSMOW}}} - 1 \quad (1)$$

We used Igor Pro software (WaveMetrics Inc., Lake Oswego OR, USA) to derive O isotope enrichment factors, ε_O, with a nonlinear least-squares regression according to eq 2, where δ¹⁸O and δ¹⁸O₀ are O isotope signatures determined in samples from oxygen isotope fractionation experiments and in standards, respectively. *c/c*₀ is the fraction of remaining aqueous O₂.

$$\frac{\delta^{18}\text{O} + 1}{\delta^{18}\text{O}_0 + 1} = (c/c_0)^{\epsilon_0} \quad (2)$$

Average ¹⁸O-kinetic isotope effects (¹⁸O-KIE) of both O atoms were determined with eq 3.^{41,51} Uncertainties of ε_O and ¹⁸O-KIEs are reported as 95% confidence intervals.

$$^{18}\text{O-KIE} = \frac{1}{1 + \epsilon_0} \quad (3)$$

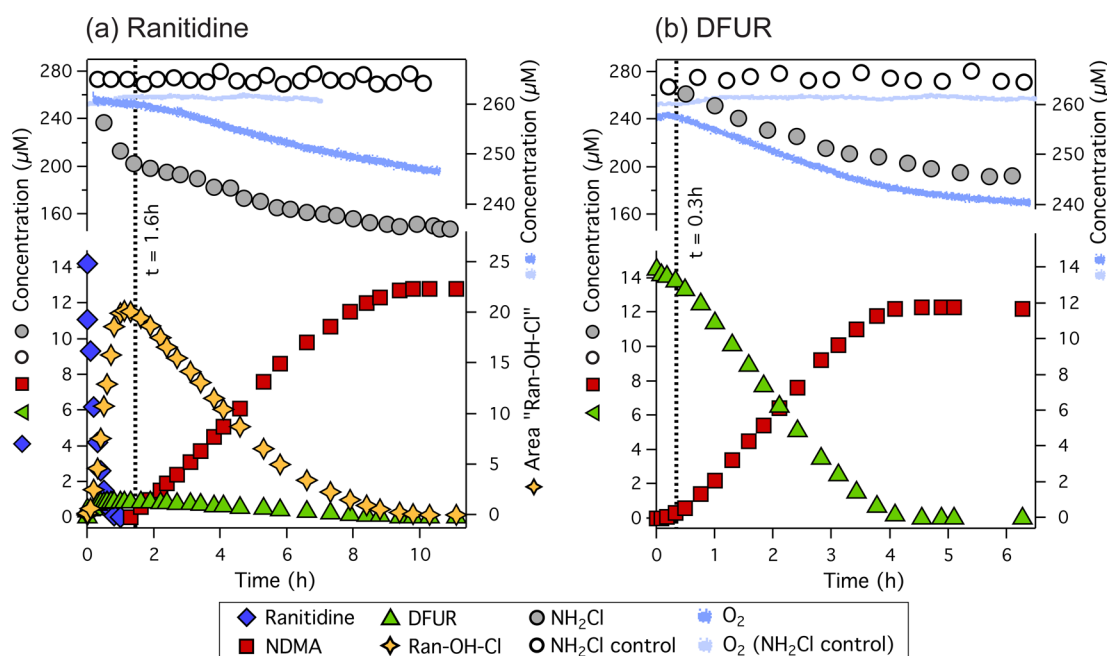


Figure 1. NDMA formation during the reaction of NH_2Cl ($270 \mu\text{M}$) with (a) ranitidine ($15 \mu\text{M}$) over 11 h and (b) DFUR ($15 \mu\text{M}$) over 6.5 h in 10 mM phosphate buffer at pH 8.0. Consumption of NH_2Cl (measured with MIMS) and aqueous O_2 is depicted as gray circles and light blue line, respectively. Note break in y-axes and scale change.

RESULTS AND DISCUSSION

Chloramination of Amines: Kinetics, Reaction Products, and Stoichiometry of NH_2Cl and O_2 Consumption.

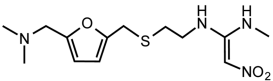
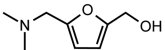
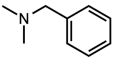
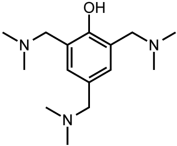
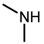
Chloramination of Ranitidine. The reaction of ranitidine ($15 \mu\text{M}$) with NH_2Cl ($270 \mu\text{M}$) at pH 8.0 produced NDMA with a molar yield of $89.9 \pm 0.1\%$ in agreement with previous observations.^{8,26–28} Figure 1a shows the kinetics of the disappearance of ranitidine, dissolved O_2 , and NH_2Cl as well as the formation of NDMA. Within 1 h, ranitidine was depleted following pseudo-first-order kinetics (Figure S8). The second-order rate constant for the reaction of ranitidine with NH_2Cl was $6.1 \pm 0.3 \text{ M}^{-1} \text{ s}^{-1}$ in agreement with a previous study.²⁸

The formation of NDMA only started after 1.6 h (dashed vertical line in Figure 1a) when ranitidine had disappeared completely suggesting the presence of a critical intermediate. Indeed, NDMA formation was concomitant with the decline of a transient reaction product (yellow stars, Figure 1a) with $m/z [\text{M} + \text{H}^+] = 365.1049$ corresponding to the molecular formula $\text{C}_{13}\text{H}_{21}\text{N}_4\text{O}_4\text{SCl}$. We report this intermediate with arbitrary peak areas due to the lack of standard materials. The mass of $\text{C}_{13}\text{H}_{21}\text{N}_4\text{O}_4\text{SCl}$ exceeds that of ranitidine ($m/z [\text{M} + \text{H}^+] = 315.1485$) by 50 Da, which corresponds to the presence of an additional hydroxyl group (+OH), an additional Cl atom (+Cl), and a loss of 2 hydrogen atoms (−2H). The intermediate, which we refer to as Ran-OH-Cl, was identified in a previous study for the chloramination of ranitidine under similar experimental conditions.²⁹ MS/MS fragmentation patterns of Ran-OH-Cl suggest that the 2-(dimethylamino)methylfuran moiety remained intact during chloramination (Figure S15). Apparently, chlorination and hydroxylation of ranitidine occurred more rapidly at the thioethyl-*N*-methyl-2-nitroethene-1,1-diamine moiety than at the 2-(dimethylamino)-methylfuran group. Note that we measured only minor concentrations of 5-(dimethylaminomethyl)furfuryl alcohol (DFUR, $m/z [\text{M} + \text{H}^+] = 156.1021$, Figure 1a), a known NDMA precursor.²⁷ Small amounts of DFUR as well as the

coincidence of NDMA formation with the disappearance of Ran-OH-Cl suggest that the latter was the primary NDMA precursor during chloramination of ranitidine.

The concentration trends of NH_2Cl and O_2 reveal that the transformation of ranitidine within the first 1.6 h involved NH_2Cl , but not dissolved O_2 because its concentration remained constant until ranitidine disappeared. In contrast, the disappearance of Ran-OH-Cl and the concomitant formation of NDMA after 1.6 h were accompanied by a decline in NH_2Cl and O_2 concentration (Figure 1a). The total amount of consumed NH_2Cl during chloramination of ranitidine amounted to $124 \pm 2 \mu\text{M}$ corresponding to 8.7 ± 0.2 times the initial ranitidine concentration (Table 1). NH_2Cl consumption rates were distinctly different before and after 1.6 h and enabled us to attribute the loss of NH_2Cl to the transformation of ranitidine vs the formation of NDMA (Figure S9a). To compare the two kinetic regimes, we report operational pseudo-first-order rate constants for the consumption of NH_2Cl . During the transformation of ranitidine, $60.5 \mu\text{M}$ NH_2Cl were consumed with a rate constant $k_{\text{obs},1}^{\text{NH}_2\text{Cl}}$ of $(7.2 \pm 0.5) \cdot 10^{-5} \text{ s}^{-1}$. This share of NH_2Cl consumption equaled 4.3 times the initial ranitidine concentration. The overstoichiometric NH_2Cl consumption suggests that multiple sites of the thioethyl-*N*-methyl-2-nitroethene-1,1-diamine moiety (e.g., S and N atoms) were chlorinated as suggested previously by Le Roux et al.²⁹ During the formation of NDMA, $63 \mu\text{M}$ NH_2Cl were consumed corresponding to 4.4 times the initial ranitidine concentration (Table 1). The rate constant of NH_2Cl consumption ($k_{\text{obs},2}^{\text{NH}_2\text{Cl}} = (1.1 \pm 0.04) \cdot 10^{-5} \text{ s}^{-1}$) was 7-fold smaller than the one observed during transformation of ranitidine implying differing reactions of NH_2Cl with ranitidine and reaction intermediates such as Ran-OH-Cl, respectively. The overstoichiometric NH_2Cl consumption during NDMA formation indicates that NH_2Cl might be involved in several reactions of the multistep NDMA formation pathway. Experiments with differing ranitidine to NH_2Cl ratios underscore the

Table 1. NDMA Formation from the Reaction of Ranitidine, 5-(Dimethylaminomethyl)furfuryl alcohol (DFUR), *N,N*-Dimethylbenzylamine (DMBA), 2,4,6-Tris(dimethylaminomethyl)phenol (TDMAP), and Dimethylamine (DMA) with NH_2Cl in 10 mM Phosphate Buffer at pH 8.0 in the Presence and Absence of *t*-BuOH, ABTS, and Trolox. Molecular Structure of the Precursors, Molar NDMA Yields, Stoichiometries of the Reaction of $\text{N}(\text{CH}_3)_2$ -groups, Dissolved O_2 , and NH_2Cl , as well as ^{18}O Kinetic Isotope Effects (^{18}O -KIEs).

precursor	molecular structure	NDMA yield ^a (%)	molar reaction stoichiometry ^b $\text{N}(\text{CH}_3)_2\text{-group} : \text{O}_2^c : \text{NH}_2\text{Cl}^c$	^{18}O -KIE (-)
Ranitidine		89.9 ± 0.1	$1.0 : 1.0 : 8.7^d (4.4^e)$	1.0061 ± 0.0004
+ <i>t</i> -BuOH (40 mM)		87.8 ± 0.2	n.m. ^f : n.m. : 6.6^d	
DFUR		84.6 ± 0.4	$1.0 : 1.1 : 4.7$	1.0060 ± 0.0006
+ <i>t</i> -BuOH (40 mM)		80.6 ± 0.1	n.m. ^f : n.m. : 4.0	
+ ABTS (2 mM)		$<0.7^g$	0.9 : 0 : 16	
+ trolox (0.5 mM)		$<0.7^g$	0.12 : n.m. ^f : 7.5	
DMBA		82.5 ± 0.2	$1.0^h : 1.1 : 4.7$	1.0026 ± 0.0003
TDMAP		15.8 ± 0.01	$1.0^h : 1.0 : 3.9$	1.0092 ± 0.0009
DMA		1.4 ± 0.1	$1.0^h : >0.6^i : 2.2$	1.0077 ± 0.0012

^aPer $\text{N}(\text{CH}_3)_2$ -group of the precursor. ^bConcentration of removed $\text{N}(\text{CH}_3)_2$ -groups, O_2 , and NH_2Cl at the end of the experiment relative to the initial concentration of $\text{N}(\text{CH}_3)_2$ -groups of the precursor compound. ^cUncertainties are $\pm(0.1-0.2)$. ^dOverall NH_2Cl consumption. ^e NH_2Cl consumption associated with formation of NDMA. ^fn.m. = not measured. ^gBelow the detection limit of NDMA in aqueous samples ($<0.1 \mu\text{M}$). ^hNominal initial concentration of $\text{N}(\text{CH}_3)_2$ -groups. ⁱDetermined after approximately 50% of the total reaction time (Figure S11).

importance of NH_2Cl because maximum NDMA yields from ranitidine were only reached in the presence of ≥ 15 -fold excess of NH_2Cl (Figure S7).

In contrast to overstoichiometric NH_2Cl consumption, we observed a stoichiometric disappearance of dissolved O_2 during the formation of NDMA. After 10 h, NDMA formation was complete and the amount of consumed O_2 ($14.3 \pm 0.3 \mu\text{M}$) matched the initial concentration of ranitidine ($14.2 \pm 0.1 \mu\text{M}$) within analytical uncertainty. The stoichiometries of O_2 and NH_2Cl consumption are compiled in Tables 1 and S1. To assess whether the molar reaction stoichiometry determined in the ranitidine experiment also applies for other amine-containing NDMA precursors, we chloraminated two tertiary amines, which are known to produce high molar NDMA yields, namely DFUR and *N,N*-dimethylbenzylamine (DMBA) as well as 2,4,6-tris(dimethylaminomethyl)phenol (TDMAP) and dimethylamine (DMA), which are known to produce significantly lower molar NDMA yields.

Chloramination of Other Tertiary Amines with High Molar NDMA Yield. Chloramination of DFUR and DMBA under experimental conditions that were identical to experiments with ranitidine (pH 8.0, $270 \mu\text{M}$ NH_2Cl , Figures 1b and S10) led to high molar NDMA yields of 84.6% and 82.5%, respectively, in agreement with previously reported values.^{20,27} DFUR and DMBA are structurally similar to ranitidine and are likely transformed to NDMA by the same reaction mechanism. This

interpretation is supported by almost identical reaction stoichiometries (Table 1). The consumption of aqueous O_2 was stoichiometric ($15.2 \pm 0.3 \mu\text{M}$ vs $14.5 \mu\text{M}$ of initial DFUR concentration), while the consumption of NH_2Cl ($68.2 \pm 2.9 \mu\text{M}$) exceeded the initial DFUR concentration by a factor of 4.7 (Table 1; data for DMBA, see Table S2). To assess whether reactions of NH_2Cl with the heterocyclic ring of DFUR contributed to the overall NH_2Cl consumption, we conducted experiments with $3 \mu\text{M}$ furfuryl alcohol and $45 \mu\text{M}$ NH_2Cl under otherwise identical experimental conditions (Figure S17). No significant decrease in the NH_2Cl concentration was observed within 30 h, indicating the initial reaction of NH_2Cl and DFUR happens exclusively at the *N,N*-dimethylamine group of DFUR.

Although the molar NDMA yield and the reaction stoichiometries were almost identical for ranitidine, DFUR, and DMBA, the reaction kinetics differed significantly. Figures 1b and S10 show that NDMA formation during chloramination of DFUR and DMBA was completed within 4 and 6 h, respectively, and was thus faster than NDMA formation from ranitidine (within 10 h). During chloramination of DFUR, we observed a short lag phase within the first 0.3 h of the reaction in which only $0.3 \mu\text{M}$ of NDMA were detected. This amount is too small to lead to measurable changes of O_2 and NH_2Cl concentrations. After 0.3 h, the reaction accelerated and the formation of NDMA coincided with the disappearance of

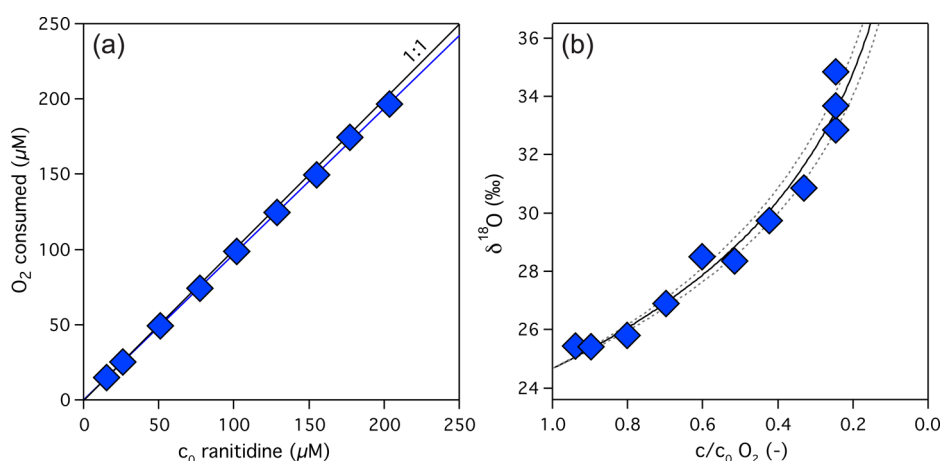


Figure 2. Reaction of ranitidine (15–200 μM) with NH_2Cl (3 mM) in 10 mM phosphate buffer at pH 8.0. (a) Consumption of aqueous O_2 after completion of the chloramination reactions vs initial concentration, c_0 , of ranitidine. (b) Oxygen isotope fractionation shown as changes of $\delta^{18}\text{O}$ -values in aqueous O_2 vs fraction of remaining O_2 (c/c_0). The solid line represents the nonlinear least-squares regression with eq 2, and dashed lines are 95% confidence intervals of the fit.

DFUR, O_2 , and NH_2Cl (Figure S8b). NH_2Cl was consumed with a pseudo-first-order rate constant of $(2.2 \pm 0.1) \cdot 10^{-5} \text{ s}^{-1}$, which is twice the $k_{\text{obs}, 2}^{\text{NH}_2\text{Cl}}$ observed during NDMA formation from ranitidine. Even after NDMA formation ceased (after 4 h), the consumption of NH_2Cl continued with a smaller $k_{\text{obs}}^{\text{NH}_2\text{Cl}}$ of $(7.7 \pm 0.7) \cdot 10^{-6} \text{ s}^{-1}$ (Figure S9b). This finding suggests that some additional reactions of NH_2Cl contributed to the observed overstoichiometric NH_2Cl consumption. A tentatively identified reaction product with molecular formula $\text{C}_5\text{H}_5\text{ClO}_2$ ($m/z [\text{M} + \text{H}^+] = 133.0053$) indicates that NH_2Cl reacts with intermediates of the NDMA formation reaction leading to chlorinated furfuryl alcohol as final reaction product (for possible molecular structures, see Figure S16).

Chloramination of Tertiary and Secondary Amines with Low Molar NDMA Yield. Molar NDMA yields from chloramination of TDMAP and DMA were normalized to the number of *N,N*-dimethylamine groups of the precursor molecule and amounted to 15.8% and 1.4%, respectively. Our data is in good agreement with previously reported NDMA yields of 18.4% for TDMAP²⁰ and 1.2–2.3% for DMA.^{20,27} The kinetics of NDMA formation and concomitant NH_2Cl and O_2 consumption are shown in Figure S11. Despite significantly smaller molar NDMA yields from TDMAP and DMA, the stoichiometries of NH_2Cl and O_2 consumption were similar to the one for ranitidine, DFUR, and DMBA. The consumed amount of O_2 corresponded with the initial concentration of *N,N*-dimethylamine groups, whereas the amount of reacted NH_2Cl exceeded the initial concentrations of *N,N*-dimethylamine groups by a factor of 3.9 and 2.2 for TDMAP and DMA, respectively (Tables 1 and S2). The overstoichiometric consumption of NH_2Cl in experiments with low-yield NDMA precursors indicates that unidentified reactions other than NDMA formation likely contributed to the disappearance of NH_2Cl . The stoichiometric O_2 consumption in experiments with high- and low-yield NDMA precursors hints at the same mechanism of N atom oxygenation of secondary and tertiary amines. However, reactions with dissolved O_2 do not necessarily lead to the formation of NDMA and it is likely that other factors such as the molecular structure of the precursor molecule determine the molar NDMA yield. Note that chloramination of DMA was too slow to carry out reliable O_2 concentration measurements over the entire experiment

period (>3 days). The reported reaction stoichiometry of >0.6 in Table 1 indicates that a higher number should be expected based on an observed stoichiometric O_2 consumption in experiments with higher initial concentrations of DMA (43 μM) and NH_2Cl (1000 μM , Figure S12).

Oxygen Isotope Fractionation during the Reaction of Aqueous O_2 . To gain new insights into the reaction of O_2 during chloramination of secondary and tertiary amines, we conducted oxygen isotope analyses of aqueous O_2 . Figure 2a shows that the consumption of O_2 measured after completion of the chloramination of ranitidine was stoichiometric regardless of the initial ranitidine concentration. The same observation was made for all of the five studied organic amines (Figures S18 and S19). In these experiments, we determined the $^{18}\text{O}/^{16}\text{O}$ ratios of aqueous O_2 at natural abundance which are reported as $\delta^{18}\text{O}$ -values (eq 1). As shown for ranitidine in Figure 2b, $\delta^{18}\text{O}$ -values of aqueous O_2 increased with decreasing fraction of remaining aqueous O_2 . The observed O isotope fractionation shows that O_2 molecules containing ^{16}O reacted preferentially. The extent of O isotope fractionation was quantified with an ^{18}O -kinetic isotope effect (^{18}O -KIE, eq 3) of 1.0061 ± 0.0004 , which reflects the ratio of reaction rate constants of light and heavy O isotopes ($^{16}k_{\text{O}_2}/^{18}k_{\text{O}_2}$). In the present case, $^{16}\text{O}_2$ reacted approximately 0.6% faster than $^{16}\text{O}^{18}\text{O}$ molecules. The reaction of aqueous O_2 during the chloramination of DFUR, DMBA, TDMAP, and DMA resulted in similar ^{18}O -KIE values between 1.0026 and 1.0092 (Table 1).

The ^{18}O -KIEs found in our experiments are small compared to the range of known values of up to 1.05 for the reduction of O_2 and the activation of O_2 by enzymes and transition metal complexes.^{39–42,52–55} The magnitude of ^{18}O -KIEs is a proxy for the number of electrons transferred to O_2 as well as for the formation and cleavage of bonds to oxygen atoms in reactions up to and including the first irreversible reaction step.^{41,42} Theoretical calculations show that one and two electron reductions of O_2 to $\text{O}_2^{\bullet-}$ and $\text{O}_2^{(-II)}$ are accompanied by the largest ^{18}O isotope effects in the order of 1.03 and 1.05, respectively.^{39,40} The small ^{18}O -KIE values below 1.01 measured here for chloramination reactions imply that the disappearance of aqueous O_2 was not associated with the formation of $\text{O}_2^{\bullet-}$ and $\text{O}_2^{(-II)}$. Indeed, none of the studied

organic amines are powerful reductants that would enable the reduction of O_2 . Such an interpretation is in agreement with the previously reported lack of $O_2^{\bullet-}$ detection after addition of superoxide dismutase to the chloramination of DMA.²² Moreover, $O_2^{\bullet-}$ and $O_2^{(-II)}$ could react with organic amine precursors, chloramine, or reaction intermediates thus causing an overstoichiometric consumption of O_2 .

Much smaller ^{18}O isotope effects between 1.01 and 1.03 are known for the reversible binding of O_2 to transition-metal complexes (e.g., with Co^{II} , Cu^{II}) and the reductive activation of O_2 at enzyme active site metal centers.^{41,51,52,54,55} The smallest ^{18}O isotope effects of 1.004–1.005 have been assigned to the reversible binding of O_2 to oxygen transport proteins such as myoglobin.³⁹ These proteins have paramagnetic transition metals (e.g., Fe^{II}) in their active site, which allows binding of triplet state O_2 . The ^{18}O -KIE values associated with chloramination of amines (Table 1) are in the same range than observed for the O_2 binding to odd electron chemical species,^{39,40,53} but we exclude the presence of transition metals in our experiments. Small ^{18}O -KIE values thus suggest that the NDMA formation mechanism involves the binding of O_2 to not yet identified radical intermediates. Such elementary reactions could explain the stoichiometric disappearance of aqueous O_2 but require the presence of organic radicals, with which ground state O_2 can react in a spin allowed process. Because O_2 neither reacts with any of the organic amines nor with NH_2Cl alone, we hypothesize that radical intermediates are formed after the initial reaction of the organic amine with chloramine.

Impact of Radical Scavengers on NDMA Formation.

The presence of radical intermediates was investigated by chloramination of ranitidine and DFUR in the presence of three radical scavengers, namely *tert*-butanol (*t*-BuOH), ABTS, and trolox. Whereas *t*-BuOH served as a scavenger for hydroxyl radicals ($\bullet OH$),⁵⁶ ABTS and trolox acted as reductants of radical intermediates^{57–60} through different reaction mechanisms (see below).

As shown by the data in Table 1, *t*-BuOH did not affect the formation of NDMA. In agreement with previous studies,^{22,37} we found almost identical molar NDMA yields from the reaction of ranitidine or DFUR (both 15 μM) with NH_2Cl (225 μM) in the presence and absence of 40 mM of *t*-BuOH. Addition of *t*-BuOH did also not influence the extent of chloramine consumption (see Tables 1 and S1, Figure S20). These observations suggest that hydroxyl radicals neither contributed to the formation of NDMA nor to the consumption of NH_2Cl .⁶¹

Chloramination experiments with ABTS or trolox strongly contrast those with *t*-BuOH in that NDMA formation from DFUR was completely suppressed. In the presence of 2 mM ABTS or 0.5 mM trolox, the reaction of DFUR with NH_2Cl did not lead to the formation of NDMA over a time period of 36 h and 4 days, respectively (Figures S22 and S24). This finding contrasts the formation of >80% NDMA within 4–8 h without radical scavenger (Figures 1b and S24a). ABTS and trolox are both known to react with a wide range of reactive oxygen species including (alk)oxyl ($R-O\bullet$), nitroxyl ($N-O\bullet$), (aryl)-peroxyl ($R-O-O\bullet$), and nitryl ($N-O-O\bullet$) radicals through a one electron or H atom transfer, respectively.^{58–60,62–68} Control experiments containing radical scavengers and either DFUR or NH_2Cl showed that ABTS and trolox did not react with DFUR (Figures S22a and S24b). Reactions of ABTS and trolox with NH_2Cl were of minor relevance within the time frame of the reactions (Figures S21a and S23). Because ABTS

and trolox are weak one-electron reductants under neutral conditions ($E_H^0(ABTS^{\bullet-} + e^- \rightleftharpoons ABTS^{2-}) = 0.70$ V,⁶⁹ $E_H^0(trolox^{\bullet} + e^- + H^+ \rightleftharpoons trolox) = 0.48$ V⁷⁰), they are not oxidized by NH_2Cl . However, ABTS and trolox are known to be oxidized by radicals.^{57–60} The inhibition of NDMA formation in the presence of ABTS and trolox thus implies that the reaction intermediates from the reaction of DFUR and NH_2Cl were radicals. Similar observations regarding lower NDMA yields in the presence of trolox were made by Schreiber and Mitch³⁷ using DMA as precursor under differing experimental conditions. Furthermore, in experiments with trolox, we did no longer observe an interference at m/z 51 during MIMS measurements, which was indicative for a transient intermediate formed during chloramination of DFUR (Figure S25).

To gain additional insights into the impact of radical scavengers on the NDMA formation mechanism, we quantified the consumption of DFUR, NH_2Cl , and O_2 . In the presence of ABTS or trolox, DFUR disappeared at an approximately 15- and 8-fold smaller rate, respectively, compared to experiments without radical scavenger (Tables 1 and S1, Figure S24). The significantly retarded DFUR transformation suggests that radical scavengers reduce radical intermediates concomitant with the regeneration of DFUR. Regenerated DFUR again reacts with NH_2Cl leading to a continuous consumption of NH_2Cl until the latter is completely consumed as shown in the experiment with ABTS (Figures S21a and S22b). The amount of consumed NH_2Cl increased by a factor of 3.3 and 2.3 in the presence of ABTS and trolox, respectively (Table S1). Note that colorimetric methods for NH_2Cl quantification were impeded in the presence of ABTS. We observed, however, that ABTS was oxidized during the reaction of DFUR with NH_2Cl , which was applied in 16-fold excess (Figure S21a). The amount of oxidized ABTS equaled the initial concentration of chloramine (225 μM) after 23 h, indicating complete NH_2Cl consumption (Table S1 and Figure S21a). Aqueous O_2 measurements were unsuccessful in the presence of trolox (Figure S26), whereas the concentration of O_2 remained constant in experiments with ABTS (Table 1, Figure S21b). The constant O_2 concentration may be due to the fact that radical intermediates reacted more rapidly with ABTS than with aqueous O_2 and the former was present in excess (2 mM ABTS vs 0.25 mM O_2). An alternative explanation is that oxygen-centered peroxy radicals, formed from the reaction of radical intermediates with O_2 , were reduced back to O_2 by ABTS.

Potential NDMA Formation Mechanisms Involving Radical Intermediates. Changes of $^{18}O/^{16}O$ of aqueous O_2 as well as inhibited NDMA formation in the presence of radical scavengers point at the presence of radical intermediates in the NDMA formation mechanism. This conclusion is also in agreement with the observed NDMA formation kinetics in Figure 1. After a short lag phase, NDMA was formed concomitant with the degradation of DFUR showing that only reaction steps at the very beginning of the reaction were rate-determining, whereas later reaction steps leading to NDMA occurred almost instantaneously in agreement with fast reactions involving radical species.

Figure 3 shows a postulated mechanism for a precursor molecule with a *N,N*-dimethylamine-methylfurane structure (ranitidine, DFUR, Ran-OH-Cl; compound 1 in Figure 3) but is thought to apply likewise for other tertiary amines studied here (DMBA, TDMAP). Previous studies showed that chloramination of tertiary amines is initiated by a nucleophilic substitution reaction to a dimethylhydrazine-type compound

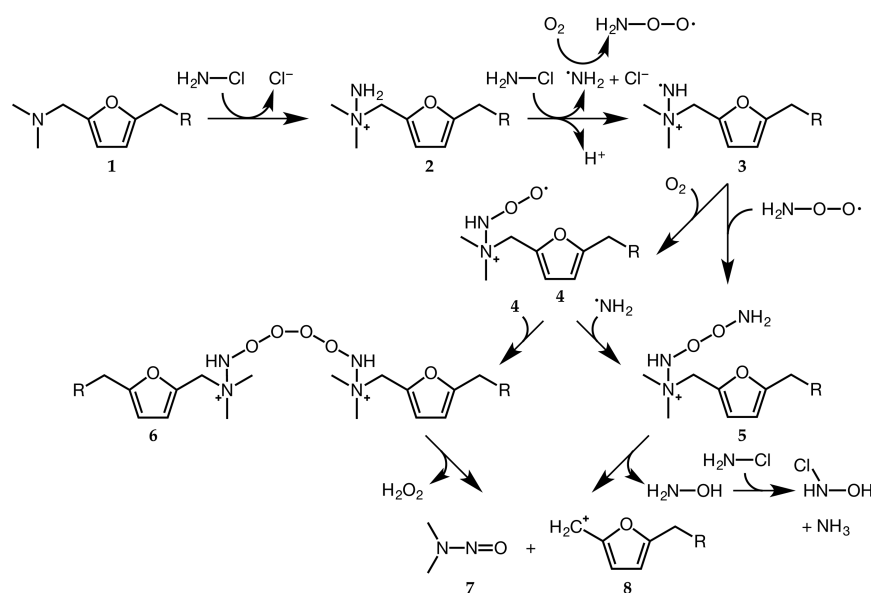


Figure 3. Hypothesized NDMA (7) formation from chloramination of *N,N*-dimethylamine-methylfuran moieties (1) through transient intermediates: substituted hydrazine (2), aminyl radicals (3 and $\text{H}_2\text{N}^\bullet$), *N*-peroxyl radicals (4). Note that decomposition of the *N*-peroxyl coupling product (6) leads to formation of 2 equivalents of NDMA and methyl-furan carbocations (8) but only one is shown here.

(2).^{29,30} Our investigation provides experimental evidence for the reaction of O_2 with transient intermediates that are likely of radical nature. The latter could be generated as aminyl radicals (3 and $\text{H}_2\text{N}^\bullet$) from the one-electron oxidation of 2 by NH_2Cl . Support for this assumption comes from observations that reactions of Fe^{2+} , phenols, or tertiary amines (e.g., chlorpromazine, aminopyrine) with chloramines lead to *N*-centered radicals at considerable rates.^{71–74} The overstoichiometric consumption of NH_2Cl during the formation of NDMA (Table 1) indicates that NH_2Cl might play an important role not only for the initial nucleophilic substitution reaction, but also for the generation of radical intermediates.

Reactions of short-lived aminyl radicals are key to rationalize the stoichiometric consumption of O_2 as well as ^{18}O -KIEs. We hypothesize that aminyl radicals such as 3 exist as *N*-centered radicals and would not be prone to typical rearrangement to carbon centered peroxy radicals because the HN^\bullet moiety is not bound to a C atom.⁷⁵ *N*-centered aminyl radicals can be oxygenated by molecular O_2 to amino-peroxyl radicals (4 and $\text{H}_2\text{N}-\text{O}-\text{O}^\bullet$) with rate constants of $10^9 \text{ M}^{-1} \text{ s}^{-1}$.^{76–78} Such a reaction of triplet O_2 is spin allowed, consistent with ^{18}O -KIEs < 1.01 , and could thus be responsible for formation of the nitroso bond of NDMA.^{39,55}

Figure 3 illustrates possible pathways leading from aminyl radical 3 to NDMA. The coupling of two *N*-peroxyl radicals 4 to compound 6 followed by the decay of 6 through the Bennett mechanism^{79,80} seems a likely option. This pathway results in the formation of two equivalents of NDMA and methyl-furfuryl carbocations (8) and one equivalent of hydrogen peroxide (H_2O_2). In separate experiments, we indeed detected H_2O_2 by adding catalase to reactors, in which $50 \mu\text{M}$ DFUR had been transformed to NDMA in the presence of $750 \mu\text{M}$ NH_2Cl (Figure S27). Upon addition of catalase, which converts two molecules of H_2O_2 to one molecule of O_2 , we measured $5.0 \pm 1.6 \mu\text{M}$ of additional O_2 , which corresponds to a H_2O_2 concentration of $7.0\text{--}13 \mu\text{M}$ at the end of the chloramination experiment (see section S13 for details). These numbers correspond to 28–52% of the theoretical maximum of $25 \mu\text{M}$

H_2O_2 assuming a stoichiometric NDMA yield from $50 \mu\text{M}$ DFUR. Because H_2O_2 was not stable when added at the beginning of a chloramination experiment (40% loss of H_2O_2 within 3.3 h, Figure S27, e.g., through partial transformation by chloramine⁸¹), we conclude that the effective concentration of H_2O_2 during NDMA formation must have been higher.

The proposed reaction pathway through species $1 \rightarrow 2 \rightarrow 3 \rightarrow 4 \rightarrow 6 \rightarrow \text{NDMA}$ is plausible based on our experimental evidence, but this interpretation strongly relies on selective coupling of amino-peroxyl radicals (4). We cannot rule out reactions of $\text{H}_2\text{N}^\bullet$ with aqueous O_2 what would lead to an overstoichiometric consumption of O_2 , except if $\text{H}_2\text{N}-\text{O}-\text{O}^\bullet$ transforms 3 to 5, from which NDMA could be cleaved off. Moreover, *N*-peroxyl radicals (4 and $\text{H}_2\text{N}-\text{O}-\text{O}^\bullet$) could decompose by alternative routes (e.g., to nitric oxide) that do not lead to NDMA but inevitably consume aqueous O_2 .⁸² If such reactions were to happen, however, one would not expect to observe the disappearance of one molecule of O_2 per *N,N*-dimethylamine group of the precursor compound (see Table 1). On the basis of the same reasoning, we consider it unlikely that nitrosating agents (e.g., nitric oxide), which would be readily oxidized by O_2 , were involved in the reactions leading to NDMA. Note that compounds like TDMA and DMA may also react along the proposed pathways to *N*-peroxyl radicals because these precursors also exhibit (near) stoichiometric O_2 consumption. However, their much smaller yields of NDMA show the importance of the molecular structure of the NDMA precursor. Whereas tertiary amines that possess an electron-rich aromatic moiety could stabilize *N*-peroxyl intermediates and lead to the formation of stable carbocationic leaving groups, these criteria might not be fulfilled in case of TDMA and secondary amines such as DMA.²⁷ Finally, the pathways shown in Figure 3 only account for the reaction of 2 to 3 equivalents of chloramine per tertiary amine while our data suggest a more than 4-fold excess of chloramine consumption (Table 1), which might be caused by side reactions leading to reaction products other than NDMA.

■ IMPLICATIONS FOR WATER TREATMENT

The radical pathway for NDMA formation, as described above, was proposed based on evidence from experiments with laboratory-grade buffer solutions containing only the organic precursors and NH_2Cl . During chloramination of source waters used for drinking water production, naturally occurring antioxidants containing, e.g., phenolic moieties, might effectively scavenge peroxy radicals,^{83,84} leading to a net decrease of NDMA formation. However, it has been shown previously that NDMA was also formed during chloramination of natural water samples that were spiked with ranitidine.⁸⁵ Compared to experiments in ultrapure water, NDMA formation was slowed down in lake and river water, presumably due to interactions of unidentified natural organic matter (NOM) components with ranitidine. However, the molar NDMA yield from ranitidine was not affected by the water matrix, indicating that reactive intermediates of the NDMA formation pathway were not scavenged by natural organic matter.⁸⁵ Indeed, it is known that the selective coupling of peroxy radicals to tetroxide species (similar to $4 \rightarrow 6$) occurs in natural water samples.^{86–88} This selective peroxy radical coupling is even exploited for the determination of $\bullet\text{OH}$ in raw waters using *t*-BuOH.^{86–88} The NDMA formation mechanism proposed here is thus also likely to be operational during chloramination of amine-containing source waters used for drinking water production.

To mitigate *N*-nitrosamine formation during full-scale water treatment, utilities using chloramine might need to implement additional treatment steps that lead to an abatement of NDMA precursors using, e.g., granular activated carbon or oxidative pretreatment with ozone.^{15,89} However, these approaches might not entirely prevent the formation of NDMA owing to varying source water qualities and the wide spectrum of precursor compounds and treatment conditions leading to NDMA.¹⁵ New methods for the identification of relevant precursors and NDMA formation pathways in source waters are required to select optimal water treatment conditions and NDMA mitigation strategies.

■ ASSOCIATED CONTENT

Supporting Information

The Supporting Information is available free of charge on the ACS Publications website at DOI: 10.1021/acs.est.6b04780.

List of all chemicals, detailed description of chemical analyses and transformation product identification, comparison of four different methods used for chloramine quantification, reactivity of DFUR with sulfite, figures illustrating (i) the impact of the precursor to chloramine ratio on molar NDMA yields, (ii) the reaction kinetics of chloramination of five NDMA precursor compounds, (iii) transformation product analysis, (iv) oxygen isotope fractionation analyses of all five precursor compounds, (v) the impact of radical scavengers on NDMA formation, and (vi) the quantification of H_2O_2 using catalase (PDF)

■ AUTHOR INFORMATION

Corresponding Author

*T. B. Hofstetter. E-mail: thomas.hofstetter@eawag.ch. Fax: +41 58 765 50 28. Phone: +41 58 765 50 76.

ORCID

Thomas B. Hofstetter: 0000-0003-1906-367X

Present Address

^{||}S.S.: Civil and Environmental Engineering, Stanford University, Stanford, CA 94305, USA

Notes

The authors declare no competing financial interest.

■ ACKNOWLEDGMENTS

This study was supported by the Swiss National Science Foundation (Project no. 200021-140545). We thank Fabian Soltermann, Rebekka Gulde, Sarah Pati, and Jakov Bolotin for analytical support as well as Michèle Heeb and Kristopher McNeill for valuable discussions.

■ REFERENCES

- (1) Andrzejewski, P.; Kasprzyk-Hordern, B.; Nawrocki, J. *N*-nitrosodimethylamine (NDMA) formation during ozonation of dimethylamine-containing waters. *Water Res.* **2008**, *42*, 863–870.
- (2) Krasner, S. W.; Mitch, W. A.; McCurry, D. L.; Hanigan, D.; Westerhoff, P. Formation, precursors, control, and occurrence of nitrosamines in drinking water: A review. *Water Res.* **2013**, *47*, 4433–4450.
- (3) Mitch, W. A.; Sedlak, D. L. Factors controlling nitrosamine formation during wastewater chlorination. *Water Sci. Technol.* **2002**, *2*, 191–198.
- (4) Russell, C. G.; Blute, N. K.; Via, S.; Wu, X.; Chowdhury, Z. Nationwide assessment of nitrosamine occurrence and trends. *J. Am. Water Works Assoc.* **2012**, *104*, 205–217.
- (5) Zimmermann, S. G.; Wittenwiler, M.; Hollender, J.; Krauss, M.; Ort, C.; Siegrist, H.; von Gunten, U. Kinetic assessment and modeling of an ozonation step for full-scale municipal wastewater treatment: Micropollutant oxidation, by-product formation and disinfection. *Water Res.* **2011**, *45*, 605–617.
- (6) Lee, C.; Schmidt, C.; Yoon, J.; von Gunten, U. Oxidation of *N*-nitrosodimethylamine (NDMA) precursors with ozone and chlorine dioxide: Kinetics and effect on NDMA formation potential. *Environ. Sci. Technol.* **2007**, *41*, 2056–2063.
- (7) Park, S.-H.; Wei, S.; Mizaikoff, B.; Taylor, A. E.; Favero, C.; Huang, C.-H. Degradation of amine-based water treatment polymers during chloramination as *N*-nitrosodimethylamine (NDMA) precursors. *Environ. Sci. Technol.* **2009**, *43*, 1360–1366.
- (8) Shen, R.; Andrews, S. A. Demonstration of 20 pharmaceuticals and personal care products (PPCPs) as nitrosamine precursors during chloramine disinfection. *Water Res.* **2011**, *45*, 944–952.
- (9) Oya, M.; Kosaka, K.; Asami, M.; Kunikane, S. Formation of *N*-nitrosodimethylamine (NDMA) by ozonation of dyes and related compounds. *Chemosphere* **2008**, *73*, 1724–1730.
- (10) Xu, B.; Qin, C.; Hu, C.-Y.; Lin, Y.-L.; Xia, S.-J.; Xu, Q.; Mwakaganda, S. A.; Bi, X.; Gao, N.-Y. Degradation kinetics and *N*-nitrosodimethylamine formation during monochloramination of chlortoluron. *Sci. Total Environ.* **2012**, *417–418*, 241–247.
- (11) Chen, Z.; Valentine, R. L. The influence of the pre-oxidation of natural organic matter on the formation of *N*-nitrosodimethylamine (NDMA). *Environ. Sci. Technol.* **2008**, *42*, 5062–5067.
- (12) Schmidt, C. K.; Brauch, H.-J. *N,N*-Dimethylsulfamide as precursor for *N*-nitrosodimethylamine (NDMA) formation upon ozonation and its fate during drinking water treatment. *Environ. Sci. Technol.* **2008**, *42*, 6340–6346.
- (13) Wert, E. C.; Rosario-Ortiz, F. L. Intracellular organic matter from cyanobacteria as a precursor for carbonaceous and nitrogenous disinfection byproducts. *Environ. Sci. Technol.* **2013**, *47*, 6332–6340.
- (14) Selbes, M.; Kim, D.; Karanfil, T. The effect of pre-oxidation on NDMA formation and the influence of pH. *Water Res.* **2014**, *66*, 169–179.
- (15) McCurry, D. L.; Krasner, S. W.; von Gunten, U.; Mitch, W. A. Determinants of disinfectant pretreatment efficacy for nitrosamine control in chloraminated drinking water. *Water Res.* **2015**, *84*, 161–170.

- (16) Shah, A. D.; Krasner, S. W.; Lee, C. F. T.; von Gunten, U.; Mitch, W. A. Trade-offs in disinfection byproduct formation associated with precursor preoxidation for control of *N*-nitrosodimethylamine formation. *Environ. Sci. Technol.* **2012**, *46*, 4809–4818.
- (17) Krasner, S. W.; Lee, C. F. T.; Mitch, W. A.; von Gunten, U. *Development of a bench-scale test to predict the formation of nitrosamines*; Water Research Foundation: Denver, 2012.
- (18) Choi, J.; Valentine, R. L. Formation of *N*-nitrosodimethylamine (NDMA) from reaction of monochloramine: A new disinfection by-product. *Water Res.* **2002**, *36*, 817–824.
- (19) Shah, A. D.; Mitch, W. A. Halonitroalkanes, halonitriles, haloamides, and *N*-nitrosamines: A critical review of nitrogenous disinfection byproduct formation pathways. *Environ. Sci. Technol.* **2012**, *46*, 119–131.
- (20) Le Roux, J.; Gallard, H.; Croué, J.-P. Formation of NDMA and halogenated DBPs by chloramination of tertiary amines: The influence of bromide ion. *Environ. Sci. Technol.* **2012**, *46*, 1581–1589.
- (21) Mitch, W. A.; Sedlak, D. L. Characterization and fate of *N*-nitrosodimethylamine precursors in municipal wastewater treatment plants. *Environ. Sci. Technol.* **2004**, *38*, 1445–1454.
- (22) Schreiber, I. M.; Mitch, W. A. Nitrosamine formation pathway revisited: The importance of chloramine speciation and dissolved oxygen. *Environ. Sci. Technol.* **2006**, *40*, 6007–6014.
- (23) Shen, R.; Andrews, S. A. NDMA formation from amine-based pharmaceuticals - Impact from prechlorination and water matrix. *Water Res.* **2013**, *47*, 2446–2457.
- (24) Padhye, L. P.; Kim, J.-H.; Huang, C.-H. Oxidation of dithiocarbamates to yield *N*-nitrosamines by water disinfection oxidants. *Water Res.* **2013**, *47*, 725–736.
- (25) Mitch, W. A.; Schreiber, I. M. Degradation of tertiary alkylamines during chlorination/chloramination: Implications for formation of aldehydes, nitriles, halonitroalkanes, and nitrosamines. *Environ. Sci. Technol.* **2008**, *42*, 4811–4817.
- (26) Le Roux, J.; Gallard, H.; Croué, J.-P. Chloramination of nitrogenous contaminants (pharmaceuticals and pesticides): NDMA and halogenated DBPs formation. *Water Res.* **2011**, *45*, 3164–3174.
- (27) Selbes, M.; Kim, D.; Ates, N.; Karanfil, T. The roles of tertiary amine structure, background organic matter and chloramine species on NDMA formation. *Water Res.* **2013**, *47*, 945–953.
- (28) Spahr, S.; Bolotin, J.; Schleucher, J.; Ehlers, I.; von Gunten, U.; Hofstetter, T. B. Compound-specific carbon, nitrogen, and hydrogen isotope analysis of *N*-nitrosodimethylamine in aqueous solutions. *Anal. Chem.* **2015**, *87*, 2916–2924.
- (29) Le Roux, J.; Gallard, H.; Croué, J.-P.; Papot, S.; Deborde, M. NDMA formation by chloramination of ranitidine: Kinetics and mechanisms. *Environ. Sci. Technol.* **2012**, *46*, 11095–11103.
- (30) Liu, Y. D.; Selbes, M.; Zeng, C.; Zhong, R.; Karanfil, T. Formation mechanism of NDMA from ranitidine, trimethylamine, and other tertiary amines during chloramination: A computational study. *Environ. Sci. Technol.* **2014**, *48*, 8653–8663.
- (31) Taube, H. Mechanisms of oxidation with oxygen. *J. Gen. Physiol.* **1965**, *49*, 29–50.
- (32) Valentine, J. S.; Foote, C. S.; Greenberg, A.; Liebman, J. F. *Active Oxygen in Biochemistry*; SEARCH Series, Vol. 3; Springer: The Netherlands, 1995.
- (33) Foote, C. S.; Valentine, J. S.; Greenberg, A.; Liebman, J. F. *Active Oxygen in Chemistry*; SEARCH Series, Vol. 2; Springer: The Netherlands, 1995.
- (34) Kearns, D. R. Physical and chemical properties of singlet molecular oxygen. *Chem. Rev.* **1971**, *71*, 395–427.
- (35) Valentine, J. S. Dioxygen reactions. In *Bioinorganic Chemistry*; Bertini, I., Gray, H. B., Lippard, S. J., Valentine, J. S., Eds.; University Science Books: Mill Valley, CA, 1994; pp 253–314.
- (36) Armstrong, D. A.; Huie, R. E.; Koppenol, W. H.; Lymar, S. V.; Merényi, G.; Neta, P.; Ruscic, B.; Stanbury, D. M.; Steenken, S.; Wardman, P. Standard electrode potentials involving radicals in aqueous solution: Inorganic radicals (IUPAC Technical Report). *Pure Appl. Chem.* **2015**, *87*, 1139–1150.
- (37) Schreiber, I. M.; Mitch, W. A. Enhanced nitrogenous disinfection byproduct formation near the breakpoint: Implications for nitrification control. *Environ. Sci. Technol.* **2007**, *41*, 7039–7046.
- (38) Kemper, J. M.; Walse, S. S.; Mitch, W. A. Quaternary amines as nitrosamine precursors: A role for consumer products? *Environ. Sci. Technol.* **2010**, *44*, 1224–1231.
- (39) Tian, G.; Klinman, J. P. Discrimination between ^{16}O and ^{18}O in oxygen binding to the reversible oxygen carriers hemoglobin, myoglobin, hemerythrin, and hemocyanin: A new probe for oxygen binding and reductive activation by proteins. *J. Am. Chem. Soc.* **1993**, *115*, 8891–8897.
- (40) Roth, J. P.; Klinman, J. P. Oxygen-18 isotope effects as a probe of enzymatic activation of molecular oxygen. In *Isotope Effects in Chemistry and Biology*; Kohen, A., Limbach, H.-H., Eds.; CRC Press/Taylor & Francis: New York, 2006; pp 645–669.
- (41) Ashley, D. C.; Brinkley, D. W.; Roth, J. P. Oxygen isotope effects as structural and mechanistic probes in inorganic oxidation chemistry. *Inorg. Chem.* **2010**, *49*, 3661–3675.
- (42) Roth, J. P. Oxygen isotope effects as probes of electron transfer mechanisms and structures of activated O_2 . *Acc. Chem. Res.* **2009**, *42*, 399–408.
- (43) Valentine, R. L.; Brandt, K. I.; Jafvert, C. T. A spectrophotometric study of the formation of an unidentified monochloramine decomposition product. *Water Res.* **1986**, *20*, 1067–1074.
- (44) Soltermann, F.; Lee, M.; Canonica, S.; von Gunten, U. Enhanced *N*-nitrosamine formation in pool water by UV irradiation of chlorinated secondary amines in the presence of monochloramine. *Water Res.* **2013**, *47*, 79–90.
- (45) Pati, S. G.; Bolotin, J.; Brennwald, M. S.; Kohler, H.-P. E.; Werner, R. A.; Hofstetter, T. B. Measurement of oxygen isotope ratios ($^{18}\text{O}/^{16}\text{O}$) of aqueous O_2 in small samples by gas chromatography isotope ratio mass spectrometry (GC/IRMS). *Rapid Commun. Mass Spectrom.* **2016**, *30*, 684–690.
- (46) Gulde, R.; Meier, U.; Schymanski, E. L.; Kohler, H.-P. E.; Helbling, D. E.; Derrer, S.; Rentsch, D.; Fenner, K. Systematic exploration of biotransformation reactions of amine-containing micropollutants in activated sludge. *Environ. Sci. Technol.* **2016**, *50*, 2908–2920.
- (47) Soltermann, F.; Widler, T.; Canonica, S.; von Gunten, U. Comparison of a novel extraction-based colorimetric (ABTS) method with membrane introduction mass spectrometry (MIMS): Trichloramine dynamics in pool waters. *Water Res.* **2014**, *58*, 258–268.
- (48) Pinkernell, U.; Nowack, B.; Gallard, H.; von Gunten, U. Methods for the photometric determination of reactive bromine and chlorine species with ABTS. *Water Res.* **2000**, *34*, 4343–4350.
- (49) Eaton, A. D.; Clesceri, L. S.; Rice, E. W.; Greenberg, A. E. *Standard Methods for the Examination of Water and Wastewater*, 21st ed.; American Public Health Association, American Water Works Association, and Water Environment Federation, 2005.
- (50) Harp, D. L. Specific determination of inorganic monochloramine in chlorinated wastewaters. *Water Environ. Res.* **2000**, *72*, 706–713.
- (51) Francisco, W. A.; Tian, G.; Fitzpatrick, P. F.; Klinman, J. P. Oxygen-18 kinetic isotope effect studies of the tyrosine hydroxylase reaction: Evidence of rate limiting oxygen activation. *J. Am. Chem. Soc.* **1998**, *120*, 4057–4062.
- (52) Lanci, M. P.; Roth, J. P. Oxygen isotope effects upon reversible O_2 -binding reactions: Characterizing mononuclear superoxide and peroxide structures. *J. Am. Chem. Soc.* **2006**, *128*, 16006–16007.
- (53) Roth, J. P. Advances in studying bioinorganic reaction mechanisms: Isotopic probes of activated oxygen intermediates in metalloenzymes. *Curr. Opin. Chem. Biol.* **2007**, *11*, 142–150.
- (54) Stahl, S. S.; Francisco, W. A.; Merks, M.; Klinman, J. P.; Lippard, S. J. Oxygen kinetic isotope effects in soluble methane monooxygenase. *J. Biol. Chem.* **2001**, *276*, 4549–4553.
- (55) Mirica, L. M.; McCusker, K. P.; Munos, J. W.; Liu, H.; Klinman, J. P. ^{18}O kinetic isotope effects in non-heme iron enzymes: Probing the nature of Fe/O_2 intermediates. *J. Am. Chem. Soc.* **2008**, *130*, 8122–8123.

- (56) Elovitz, M. S.; von Gunten, U. Hydroxyl radical/ozone ratios during ozonation processes. I. The R_{ct} concept. *Ozone: Sci. Eng.* **1999**, *21*, 239–260.
- (57) Yim, M. B.; Chock, P. B.; Stadtman, E. R. Enzyme function of copper, zinc superoxide-dismutase as a free-radical generator. *J. Biol. Chem.* **1993**, *268*, 4099–4105.
- (58) Alberto, M. E.; Russo, N.; Grand, A.; Galano, A. A physicochemical examination of the free radical scavenging activity of Trolox: Mechanism, kinetics and influence of the environment. *Phys. Chem. Chem. Phys.* **2013**, *15*, 4642–4650.
- (59) Neta, P.; Huie, R. E.; Ross, A. B. Rate constants for reactions of peroxy radicals in fluid solutions. *J. Phys. Chem. Ref. Data* **1990**, *19*, 413–513.
- (60) Gębicki, J. L.; Maciejewska, M. Reactions of 2,2'-azinobis-(3-ethylbenzthiazoline-6-sulfonate) dianion, ABTS^{2-} , with $\bullet\text{OH}$, $(\text{SCN})_2^{\bullet-}$, and glycine or valine peroxy radicals. *J. Phys. Chem. A* **2007**, *111*, 2122–2127.
- (61) Poskrebyshev, G. A.; Huie, R. E.; Neta, P. Radiolytic reactions of monochloramine in aqueous solutions. *J. Phys. Chem. A* **2003**, *107*, 7423–7428.
- (62) Bartosz, G.; Janaszewska, A.; Ertel, D.; Bartosz, M. Simple determination of peroxy radical-trapping capacity. *IUBMB Life* **1998**, *46*, 519–528.
- (63) Goldstein, S.; Czapski, G. Kinetics of nitric-oxide autoxidation in aqueous solution in the absence and presence of various reductants. The nature of the oxidizing intermediates. *J. Am. Chem. Soc.* **1995**, *117*, 12078–12084.
- (64) Elia, P.; Azoulay, A.; Zeiri, Y. On the efficiency of water soluble antioxidants. *Ultrason. Sonochem.* **2012**, *19*, 314–324.
- (65) Priyadarsini, K. I.; Kapoor, S.; Naik, D. B. One- and two-electron oxidation reactions of trolox by peroxyxynitrite. *Chem. Res. Toxicol.* **2001**, *14*, 567–571.
- (66) Bisby, R. H.; Morgan, C. G.; Hamblett, I.; Gorman, A. A. Quenching of singlet oxygen by Trolox C, ascorbate, and amino acids: Effects of pH and temperature. *J. Phys. Chem. A* **1999**, *103*, 7454–7459.
- (67) Pattison, D. I.; Davies, M. J.; Asmus, K.-D. Absolute rate constants for the formation of nitrogen-centred radicals from chloramines/amides and their reactions with antioxidants. *J. Chem. Soc., Perkin Trans. 2* **2002**, 1461–1467.
- (68) Aliaga, C.; Lissi, E.; Augusto, O.; Linares, E. Kinetics and mechanism of the reaction of a nitroxide radical (Tempol) with a phenolic antioxidant. *Free Radical Res.* **2003**, *37*, 225–230.
- (69) Sander, M.; Hofstetter, T. B.; Gorski, C. A. Electrochemical analyses of redox-active iron minerals: a review of nonmediated and mediated approaches. *Environ. Sci. Technol.* **2015**, *49*, 5862–5878.
- (70) Steenken, S.; Neta, P. One-electron redox potentials of phenols. Hydroxy- and aminophenols and related compounds of biological interest. *J. Phys. Chem.* **1982**, *86*, 3661–3667.
- (71) Vikesland, P. J.; Valentine, R. L. Modeling the kinetics of ferrous iron oxidation by monochloramine. *Environ. Sci. Technol.* **2002**, *36*, 662–668.
- (72) Vikesland, P. J.; Valentine, R. L. Reaction pathways involved in the reduction of monochloramine by ferrous iron. *Environ. Sci. Technol.* **2000**, *34*, 83–90.
- (73) Heasley, V. L.; Fisher, A. M.; Herman, E. E.; Jacobsen, F. E.; Miller, E. W.; Ramirez, A. M.; Royer, N. R.; Whisenand, J. M.; Zoetewey, D. L.; Shellhamer, D. F. Investigations of the reactions of monochloramine and dichloramine with selected phenols: Examination of humic acid models and water contaminants. *Environ. Sci. Technol.* **2004**, *38*, 5022–5029.
- (74) Kalyanaraman, B.; Sohnle, P. G. Generation of free radical intermediates from foreign compounds by neutrophil-derived oxidants. *J. Clin. Invest.* **1985**, *75*, 1618–1622.
- (75) Hawkins, C. L.; Davies, J. M. Reaction of HOCl with amino acids and peptides: EPR evidence for rapid rearrangement and fragmentation reactions of nitrogen-centred radicals. *J. Chem. Soc., Perkin Trans. 2* **1998**, *2*, 1937–1946.
- (76) Clarke, K.; Edge, R.; Johnson, V.; Land, E. J.; Navaratnam, S.; Truscott, T. G. Direct observation of $\bullet\text{NH}_2$ reactions with oxygen, amino acids, and melanins. *J. Phys. Chem. A* **2008**, *112*, 1234–1237.
- (77) Crowley, J. N.; Sodeau, J. R. Reaction between the amidogen radical, $\bullet\text{NH}_2$, and molecular-oxygen in low-temperature matrices. *J. Phys. Chem.* **1989**, *93*, 4785–4790.
- (78) Fautitano, A.; Buttafava, A.; Martinotti, F.; Bortolus, P. First electron spin resonance identification of a nitrogen peroxy radical as intermediate in the photooxidation of 2,2,6,6-tetramethylpiperidine derivatives. *J. Phys. Chem.* **1984**, *88*, 1187–1190.
- (79) Bennett, J. E.; Summers, R. Product studies of mutual termination reactions of *sec*-alkylperoxy radicals: Evidence for non-cyclic termination. *Can. J. Chem.* **1974**, *52*, 1377–1379.
- (80) Russell, G. A. Deuterium-isotope effects in the autoxidation of aralkyl hydrocarbons: Mechanism of the interaction of peroxy radicals. *J. Am. Chem. Soc.* **1957**, *79*, 3871–3877.
- (81) McKay, G.; Sjelín, B.; Chagnon, M.; Ishida, K. P.; Mezyk, S. P. Kinetic study of the reactions between chloramine disinfectants and hydrogen peroxide: Temperature dependence and reaction mechanism. *Chemosphere* **2013**, *92*, 1417–1422.
- (82) Li, J.; Blatchley, E. R., III UV photodegradation of inorganic chloramines. *Environ. Sci. Technol.* **2009**, *43*, 60–65.
- (83) Chimi, H.; Cillard, J.; Cillard, P.; Rahmani, M. Peroxy and hydroxyl radical scavenging activity of some natural phenolic antioxidants. *J. Am. Oil Chem. Soc.* **1991**, *68*, 307–312.
- (84) Nimse, S. B.; Pal, D. Free radicals, natural antioxidants, and their reaction mechanisms. *RSC Adv.* **2015**, *5*, 27986–28006.
- (85) Shen, R.; Andrews, S. A. NDMA formation kinetics from three pharmaceuticals in four water matrices. *Water Res.* **2011**, *45*, 5687–5694.
- (86) Nothe, T.; Fahlenkamp, H.; von Sonntag, C. Ozonation of wastewater: Rate of ozone consumption and hydroxyl radical yield. *Environ. Sci. Technol.* **2009**, *43*, 5990–5995.
- (87) Flyunt, R.; Leitzke, A.; Mark, G.; Mvula, E.; Reisz, E.; Schick, R.; von Sonntag, C. Determination of $\bullet\text{OH}$, $\text{O}_2^{\bullet-}$, and hydroperoxide yields in ozone reactions in aqueous solution. *J. Phys. Chem. B* **2003**, *107*, 7242–7253.
- (88) Lee, Y.; Gerrity, D.; Lee, M.; Bogeat, A. E.; Salhi, E.; Gamage, S.; Trenholm, R. A.; Wert, E. C.; Snyder, S. A.; von Gunten, U. Prediction of micropollutant elimination during ozonation of municipal wastewater effluents: Use of kinetic and water specific information. *Environ. Sci. Technol.* **2013**, *47*, 5872–5881.
- (89) Hanigan, D.; Zhang, J.; Herckes, P.; Krasner, S. W.; Chen, C.; Westerhoff, P. Adsorption of *N*-nitrosodimethylamine precursors by powdered and granular activated carbon. *Environ. Sci. Technol.* **2012**, *46*, 12630–12639.